

# Prompt-Matched Semantic Segmentation

Lingbo Liu<sup>1</sup>, Bruce X.B. Yu<sup>1</sup>, Jianlong Chang<sup>2</sup>, Qi Tian<sup>2</sup>, Chang-Wen Chen<sup>1</sup>

<sup>1</sup>The Hong Kong Polytechnic University    <sup>2</sup>Huawei Cloud & AI, Shenzhen 518000, China  
{lingbo.liu,xinboyu,changwen.chen}@polyu.edu.hk    {jianlong.chang, tian.qi1}@huawei.com

## Abstract

The objective of this work is to explore how to effectively and efficiently adapt pre-trained foundation models to various downstream tasks of image semantic segmentation. Conventional methods usually fine-tuned the whole networks for each specific dataset and it was burdensome to store the massive parameters of these networks. A few recent works attempted to insert some trainable parameters into the frozen network to learn visual prompts for efficient tuning. However, these works significantly modified the original structure of standard modules, making them inoperable on many existing high-speed inference devices, where standard modules and their parameters have been embedded. To facilitate prompt-based semantic segmentation, we propose a novel Inter-Stage Prompt-Matched Framework, which maintains the original structure of the foundation model while generating visual prompts adaptively for task-oriented tuning. Specifically, the pre-trained model is first divided into multiple stages, and their parameters are frozen and shared for all semantic segmentation tasks. A lightweight module termed Semantically-aware Prompt Matcher is then introduced to hierarchically interpolate between two stages to learn reasonable prompts for each specific task under the guidance of interim semantic maps. In this way, we can better stimulate the pre-trained knowledge of the frozen model to learn semantic concepts effectively on downstream datasets. Extensive experiments conducted on five benchmarks show that the proposed method can achieve a promising trade-off between parameter efficiency and performance effectiveness.

## Introduction

Semantic segmentation (Minaee et al. 2021) is a fundamental yet challenging problem in computer vision, which aims to automatically perform pixel-level labeling with a set of object categories for the given image. Over the past decades, this problem has attracted extensive research in industry and academia, since it can facilitate a variety of downstream applications, e.g., scene understanding (Long, Shelhamer, and Darrell 2015), satellite image analysis (Liu et al. 2022), and medical auxiliary diagnosis (He et al. 2019b).

In the literature, numerous approaches have been proposed to address semantic segmentation. In general, most previous methods first acquired a visual foundation model pre-trained on large-scale benchmarks such as ImageNet (Deng et al. 2009), and then fine-tuned the network’s param-

eters on specific downstream datasets. Two different fine-tuning strategies are typically employed in this paradigm. The first one is *full-tuning* that adjusts all parameters of the entire network. However, this strategy usually requires large amounts of training data with rich annotations and may fail to learn generalized representation when only a few labeled samples are available. Moreover, it requires to store a proprietary model with massive parameters for every segmentation task, which is expensive and unsustainable for various service platforms. For the second strategy, *head-tuning* freezes the parameters of the backbone network and only optimizes the head segmenter. Intuitively, all tasks share the same backbone and we only need to maintain an individual segmenter for each task. Despite being parameter efficient, this strategy can not well exploit the prior knowledge of the backbone to deal with complex segmentation tasks, since current pre-training tasks are usually image-level recognition, which is quite different from pixel-level segmentation. Overall, the above-mentioned strategies suffer from various issues, and we desire a more effective and efficient fine-tuning method for comprehensive semantic segmentation.

Recently, *prompt-tuning* (Liu et al. 2021) has achieved considerable results in Natural Language Processing (NLP). Some textual prompts are inserted into the downstream input to better explore the knowledge of language models. To facilitate downstream tasks in computer vision, a few works (Jia et al. 2022; Chen et al. 2022) have attempted to apply visual prompt tuning to energize the prior knowledge in those parameter-frozen foundation models. Despite some progress using only a small amount of extra parameters, these works still suffer from the following problems. **First**, they learned visual prompts in inappropriate places, i.e., either only at the input layer or at every layer. The former had limited capacity to learn effective prompts, due to the lack of direct interactions with high-level knowledge. The latter divided the foundation models unduly into many small pieces and modified their network structures, which could cause them to be unexecutable on many high-speed inference devices, especially on FPGA and ASIC (Nurvitadhi et al. 2016). In practice, many foundation models or standard modules and their trained parameters are specially embedded into these devices for high efficiency and low power consumption (Ma et al. 2017; Wang et al. 2022). It is very expensive to re-fabricate chips for those prompted models with many ad-

ditional modifications. **Second**, these works performed visual prompt tuning with limited information in a black-box mapping manner. Specifically, all previous methods only utilized the final recognition loss to optimize prompted networks and failed to learn reasonable visual prompts. It is worth noting that semantic segmentation is more challenging than image recognition, requiring richer information to perform pixel-wise inferences. Therefore, heuristic knowledge should be fully explored to generate effective visual prompts for parameter-efficient semantic segmentation.

To address the above problems, we propose an Inter-Stage Prompt-Matched Framework, which can adapt the frozen foundation model effectively to a wide range of semantic segmentation tasks. Unlike previous works that inserted learnable parameters into each layer or unit, we partition the foundation model into multiple stages and perform inter-stage prompt tuning on specific datasets. This allows those standard modules to be well maintained for efficient execution on existing FPGA and ASIC devices without any additional burdens. Moreover, a lightweight module termed Semantic-aware Prompt Matcher (SPM) is introduced to learn inter-stage visual prompts under the guidance of interim semantic maps. Specifically, the output of the previous stage is first used to generate a semantic map that provides rich prior knowledge. Then the previous output and semantic map are incorporated to adaptively learn semantic-aware prompts to generate a reasonable input for the next stage, thus better stimulating the pre-trained knowledge of the foundation model. Notice that our method is general to various backbone networks such as ResNet (He et al. 2016) and Transformer (Vaswani et al. 2017), and it can also be applied to handle widespread semantic segmentation tasks for natural, satellite, and medical images. Finally, we conduct extensive experiments on five benchmarks, and the results show that our method can achieve a promising trade-off between parameter efficiency and performance effectiveness. In particular, only optimizing SPM and the head segmenter, our method significantly outperforms *head-tuning* and is comparable to *full-tuning*.

In summary, the contributions of our work are three-fold:

- An Inter-Stage Prompt-Matched Framework is proposed to learn task-relevant visual prompts between different stages of the parameter-frozen foundation model, so that this model can be effectively adapted to various downstream tasks of semantic segmentation. Moreover, we maintain the original structure of all standard modules, thus these stages can be executed directly on those high-speed devices specially optimized for standard modules.
- A lightweight SPM is introduced to adaptively learn visual prompts between two adjacent stages. Under the guidance of the interim semantic map, the output of the previous stage can be effectively transformed into an informative input that can better energize the pre-trained knowledge of the next stage.
- Extensive experiments conducted on four benchmarks demonstrate that our method is effective and parameter-efficient for fine-tuning foundation models to various semantic segmentation tasks.

## Related Work

### Semantic Segmentation

As a typical pixel-wise prediction problem, semantic segmentation has been significantly promoted by deep neural networks. For instance, (Long, Shelhamer, and Darrell 2015) proposed Fully Convolutional Networks that replaced fully-connected layers with convolutional layers to handle images of arbitrary sizes. (Ronneberger, Fischer, and Brox 2015) applied a convolutional encoder-decoder architecture with skip connections to generate semantic maps with high resolutions. (Zhao et al. 2017) first used a backbone network to extract the feature maps of input images and then introduced a pyramid pooling module to aggregate different sub-region representations for multiscale contextual modeling. Besides the similar multiscale module, DeepLab family (Chen et al. 2015, 2017) further applied dilated convolutions to enlarge the network receptive fields and introduced Conditional Random Fields to refine the final segmentation results. (Fu et al. 2019) proposed a Dual Attention Network, which incorporated a position attention module and a channel attention module to model the spatial and channel inter-dependencies respectively. Recently, transformers (Vaswani et al. 2017) have also been applied to address this problem. One representative work is Segmenter (Strudel et al. 2021), which divided the image into local patches and fed their linear embeddings into Vision Transformer (ViT) (Dosovitskiy et al. 2020) to capture global context at each layer for semantic segmentation. Despite progress, previous methods usually fine-tuned the parameters of the whole networks respectively for each specific task of semantic segmentation. It is burdensome to store the massive parameters of these models, especially on some resource-constrained devices. In this case, we crave for a novel fine-tuning approach, where these tasks can share most of the parameters and achieve competitive results.

### Prompt Tuning

In recent years, various large-scale NLP models such as BERT (Devlin et al. 2018), GPT-3 (Brown et al. 2020), and Pangu- $\alpha$  (Zeng et al. 2021) have been developed by pre-training on huge datasets. With prompt tuning, these large-scale models achieved impressive transfer performance on myriads of downstream tasks such as translation (Tan et al. 2022), reading comprehension (Hu et al. 2022), question answering (Yang et al. 2022), etc. Inspired by the prompt tuning paradigm in NLP, it starts to attract researchers attention to diametrically use text inputs (e.g., text category label) as prompt for vision tasks (Radford et al. 2021; Jia et al. 2021). Although vision-language pre-training models achieved promising performance, this multimodal model tuning strategy requires to train a new pre-trained model and can not be smoothly applied to pre-trained vision models. With this concern, a lightweight prompt tuning paradigm VPT was proposed (Jia et al. 2022), which aims to make good use of pre-trained vision models for the downstream vision tasks. VPT represents one of initial attempts on visual prompt tuning that is either insert prompt at the input or at each layer, which does not consider the relationship be-

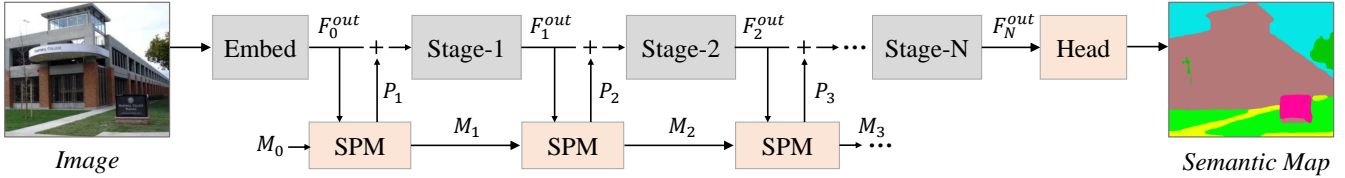


Figure 1: The architecture of the proposed Inter-Stage Prompt-Matched Framework for semantic segmentation prompt tuning. A lightweight Semantic-aware Prompt Matcher (SPM) is introduced to learn reasonable visual prompts between every two stages of the frozen backbone network. The term  $F_i^{out}$  denotes the output feature of the  $i$ -th stage, while  $P_i$  and  $M_i$  are the learned prompt map and interim semantic map generated at the  $i$ -th SPM. The symbol ‘+’ denotes the element-wise addition operation. It is worth noting that only the parameters of our SPM and head segmenter are updated during the training phase.

tween prompt stages. Following the spirit of VPT, we aim to exploit the hierarchical characteristics thereof in different stages of the pre-trained large models.

### Analogy to Adversarial Attacks

Our proposed method can be regarded as an analogy to adversarial attacks (Madry et al. 2018). Adversarial attacks attempt to fool the network by learning noise via back-propagation and combining the learned noise with the input image. Network attacks can be grouped to white-box and black-box attacks, where the former case can be deemed as an analogy to our problem since the model structure is known in advance (He, Rakin, and Fan 2019). On the contrary, it can also be analogized as a defending manner such as (Liao et al. 2018) where a denoiser is learned from the hierarchical layers of the model. Our model design is inspired by such usage of hierarchical model features.

## Methodology

### Overall Architecture

In this work, we aim to utilize vision-based prompt learning to effectively and efficiently fine-tune the pre-trained foundation model for various downstream tasks of semantic segmentation. When designing our method, we consider the following two questions: **i) where to learn visual prompts** and **ii) how to learn reasonable prompts?** We argue that previous works (Jia et al. 2022; Chen et al. 2022) are difficult to be directly applied to many existing network-embedded devices, as they inserted extra parameters into each layer or unit, which significantly modifies the original structure of the foundation model. Moreover, they only used limited information of final losses to optimize the network. Hence, their learned prompts can not well stimulate the pre-trained knowledge for the information-craving semantic segmentation. Therefore, we propose two criteria to facilitate the visual prompt tuning. **i)** We should perform prompt learning in as few places as possible to preserve the original structures of standard modules. **ii)** We should incorporate rich information to learn more effective visual prompts.

To this end, we propose an Inter-Stage Prompt-Matched Framework (see Figure 1) for semantic segmentation prompt tuning. In general, a deep semantic segmentation model consists of an universal backbone network pre-trained on large-scale datasets and a customized head segmenter with ran-

dom initialization. To reduce the number of tunable parameters, the backbone network is frozen and shared for all semantic segmentation tasks, and the head segmenter is optimized for each specific dataset. Inspired by previous NLP works (Liu et al. 2021), we apply prompt tuning to fully exploit the pre-trained visual knowledge in the frozen backbone. Different from (Jia et al. 2022; Chen et al. 2022), we propose to learn visual prompts between every two stages of the backbone network, without modifying the structures of standard modules. Specifically, the backbone network is partitioned into  $N$  standardized stages, each of which is composed of stacked standard modules, e.g., residual units or transformer units. Notice that there may be some other embedding layers before the first stage. For convenience, the output feature of the  $i$ -th stage is denoted as  $F_i^{out}$  ( $i=1, \dots, N$ ), while the output feature of those embedding layers is denoted as  $F_0^{out}$ .

We then introduce a differentiable neural network module called SPM to learn inter-stage visual prompts using a small number of parameters. As mentioned above, rich information is desired to learn semantic segmentation prompts. In this work, we find that interim semantic maps generated at intermediate layers encode the prior information of object semantics distributions, so we incorporate these semantic maps to learn reasonable prompts. Specifically, before the  $i$ -th stage, our SPM takes as inputs the feature  $F_{i-1}^{out}$  and the interim semantic map  $M_{i-1}$  of the previous stage to generate a prompt map  $P_i$  and a refined semantic map  $M_i$  simultaneously. This process can be formulated as:

$$P_i, M_i = SPM(F_{i-1}^{out}, M_{i-1}), \quad (1)$$

whose details are described in the next subsection. Notice that the initial semantic map  $M_0$  is generated from the statistic category probability. More specifically, each position on  $M_0$  is set to the probability vector of different category pixels on the training set of the downstream dataset. Then we utilize the residual mechanism to generate the prompted input  $F_i^{in}$  of the  $i$ -th stage:

$$F_i^{in} = F_{i-1}^{out} + P_i. \quad (2)$$

Thanks to the tailor-learned prompts, we can transform  $F_{i-1}^{out}$  to the more suitable input  $F_i^{in}$  for the  $i$ -th stage.

As shown in Figure 1, the proposed SPM is hierarchically inserted between different stages to jointly learn semantic-aware visual prompts. Finally, the output feature  $F_N^{out}$  of the

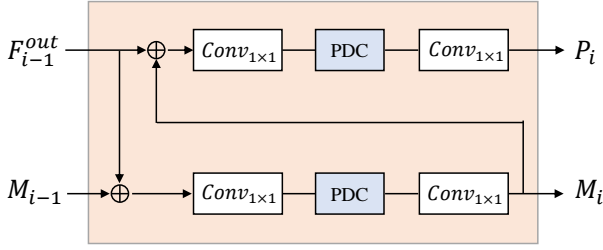


Figure 2: The architecture of our Semantic-aware Prompt Matcher.  $Conv_{1 \times 1}$  represents a convolutional layer with a kernel size of  $1 \times 1$ , while PDC denotes the Pyramid Dilation Convolution presented in Figure 3. The symbol  $\oplus$  represents the feature concatenation operation.

$N$ -th stage is fed into the head segmenter to generate the final high-quality semantic map  $M$ .

### Semantic-aware Prompt Matcher

In this subsection, we introduce the details of the proposed SPM. The purpose of this module is to integrate interim semantic maps to learn reasonable visual prompts so that the output feature of the previous stage can be transformed into a desirable input for the next stage. Here we take the SPM before the  $i$ -th stage as an example to explain our working mechanism. Specifically, the inputs of our SPM are the feature  $F_{i-1}^{out} \in \mathbb{R}^{h \times w \times c}$  and the semantic map  $M_{i-1} \in \mathbb{R}^{h \times w \times s}$  of the previous stage, where  $h$  and  $w$  are the height and width of the feature respectively.  $c$  denotes the number of feature channels, while  $s$  is the number of semantic categories.

As shown in Figure 2, our SPM consists of two parallel branches to refine the interim semantic map and generate the semantic-aware prompt. As mentioned in previous works (Zhu et al. 2019; He et al. 2019a), long-range spatial context is crucial for semantic segmentation. Therefore we introduce a Pyramid Dilation Convolution (PDC) that uses four dilated convolutional layers to capture the multi-scale long-range context. As shown in Figure 3, the input feature of PDC is divided into four sub-features along the channel dimension. The  $i$ -th sub-feature is fed into the  $i$ -th dilated convolutional layer with a kernel size of  $3 \times 3$  and a dilated rate of  $r$ . The outputs of all dilated layers are concatenated and fused using a  $1 \times 1$  convolutional layer. The proposed PDC is integrated into both branches to generate the long-range contextualized features. The details of these branches are described as follows.

**Interim Semantic Map Refinement** In general, the high-level features usually contains richer semantic information, thus we utilize the current features to generate the refined semantic map. Specifically, we first feed the concatenation of  $F_{i-1}^{out}$  and  $M_{i-1}$  into a  $1 \times 1$  convolutional layer to generate an embedded feature  $F_{i-1}^{m1} \in \mathbb{R}^{h \times w \times \hat{c}}$ , where the channel number  $\hat{c}$  is set to a small value for reducing the number of parameters. We then apply a Pyramid Dilation Convolution to obtain the long-range contextualized feature  $F_{i-1}^{m2} \in \mathbb{R}^{h \times w \times s}$ , which is further fed into a  $1 \times 1$  convolutional layer

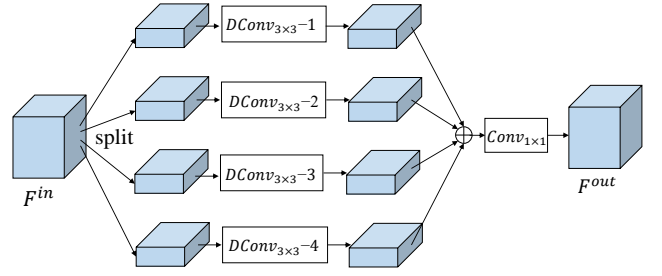


Figure 3: The structure of our Pyramid Dilation Convolution for long-range spatial context modeling.  $DConv_{3 \times 3-r}$  denotes a dilated convolutional layer with a kernel size of  $3 \times 3$  and a dilated rate of  $r$ . The input feature  $F^{in}$  and output feature  $F^{out}$  have the same dimension.

to generate the refined semantic map  $M_i \in \mathbb{R}^{h \times w \times s}$ . This process can be formulated as:

$$\begin{aligned} F_{i-1}^{m1} &= Conv_{1 \times 1}(F_{i-1}^{out} \oplus M_{i-1}), \\ F_{i-1}^{m2} &= PDC(F_{i-1}^{m1}), \\ M_i &= Softmax\{Conv_{1 \times 1}(F_{i-1}^{m2})\}, \end{aligned} \quad (3)$$

where  $\oplus$  denotes the feature concatenation operation and the  $Softmax$  layer is used to normalize the predicted scores of semantic categories.

**Semantic-aware Prompt Generation** In this branch, we incorporate the feature  $F_{i-1}^{out}$  and the refined semantic map  $M_i$  to generate the semantic-aware prompt map  $P_i \in \mathbb{R}^{h \times w \times c}$  for the next stage. As shown in Figure 2, our prompt generation branch also consists of two  $1 \times 1$  convolutional layers and a Pyramid Dilation Convolution. More specifically, similar to the attention mechanism, the final convolutional layer generates a prompt weight  $W_i^p \in \mathbb{R}^{h \times w \times c}$ , which is further applied to multiply with  $F_{i-1}^{out}$  to generate the  $P_i$ . This process can be formulated as:

$$\begin{aligned} F_{i-1}^{p1} &= Conv_{1 \times 1}(F_{i-1}^{out} \oplus M_i), \\ F_{i-1}^{p2} &= PDC(F_{i-1}^{p1}), \\ W_i^p &= Conv_{1 \times 1}(F_{i-1}^{p2}), \\ P_i &= F_{i-1}^{p1} \otimes W_i^p, \end{aligned} \quad (4)$$

where  $\otimes$  denotes the element-wise multiplication operation. Finally, we apply Eq. 2 to generate the prompted input  $F_i^{in}$  for the  $i$ -th stage.

### Network Optimization

During the training phase, the parameters of the backbone are frozen and we only update the parameters of our SPM and head segmenter on specific datasets. Finally, we use the Cross-Entropy (CE) loss function to optimize our semantic segmentation network. The total loss is defined as follows:

$$loss = CE(M, \hat{M}) + \sum_{i=1}^N a_i * CE(M_i, \hat{M}_i), \quad (5)$$

Table 1: Overview of five downstream benchmark datasets of semantic segmentation.

Dataset	#Train	#Test	#Category	Scene
ADE20K	20,210	2,000	150	natural image
Vaihingen	344	398	6	satellite image
CHASE-DB1	20	8	2	medical image
STARE	10	10		
HRF	15	30		

where  $\hat{M}$  is the ground-truth semantic map and  $M$  is our final semantic map predicted by the head segmenter.  $a_i$  is the loss weight of the  $i$ -th interim semantic map.

## Experiment

In this section, we first introduce the downstream datasets of semantic segmentation. We then compare the proposed method with common fine-tuning approaches on these datasets. Finally, we conduct ablation studies to verify the effectiveness of each component in our method.

### Semantic Segmentation Datasets

We conduct extensive experiments on five semantic segmentation datasets of various scenarios, including ADE20K (Zhou et al. 2017), Vaihingen<sup>1</sup>, CHASE-DB1 (Fraz et al. 2012), STARE (Hoover, Kouznetsova, and Goldbaum 2000) and HRF (Budai et al. 2013). The overview of these datasets is summarized in Table 1. Some examples of these datasets are visualized in Figure 4.

- **ADE20K.** It is a large-scale scene parsing benchmark with 150 object and stuff classes. The public ADE20K dataset consists of 20,210 images for training and 2,000 images for validation. This dataset is challenging due to the high intra-class variance and low inter-class variance. Moreover, the objects suffers from great scale variations.
- **Vaihingen.** It is a medium-scale dataset for satellite image segmentation. This dataset consists of six types of semantic object, e.g., buildings, streets, cars, etc. The training set contains 344 images, while the testing set has 398 images. All images has the same resolution  $512 \times 512$ .
- **CHASE-DB1, STARE, HRF.** They are few-shot medical image segmentation datasets that aim to segment retinal vessels from background. These datasets consist of the eye fundus images of some healthy patients and some patients with representative eye diseases. These images have higher resolutions, e.g.,  $999 \times 960$  for CHASE-DB1,  $700 \times 605$  for STARE,  $3504 \times 2336$  for HRF.

### Comparison with Common Fine-tuning Methods

Here we compare the proposed method with three common approaches, i.e., *full-tuning*, *head-tuning* and *learn-from-scratch*. The overall experimental settings are as follows:

- **Backbone Network.** All methods adopt ResNet-101 (He et al. 2016) as the backbone. Except *learn-from-scratch*,

<sup>1</sup><https://www.isprs.org/education/benchmarks/UrbanSemLab/2d-sem-label-vaihingen.aspx>

Table 2: Performance of different methods on the ADE20K dataset for natural image segmentation, when the backbone network is ResNet-101 pre-trained on ImageNet.

Method	Trainable Parameters (M)			mIoU $\uparrow$
	Backbone	Prompt	Head	
Full-Tuning	42.41	0	23.15	43.96
Learn from Scratch	42.41	0	23.15	34.84
Head-Tuning	0	0	23.15	34.08
Ours	0	3.11	23.15	40.01

Table 3: Performance of different methods on the Vaihingen dataset for satellite image segmentation, when the backbone network is ResNet-101 pre-trained on ImageNet.

Method	Trainable Parameters (M)			mIoU $\uparrow$
	Backbone	Prompt	Head	
Full-Tuning	42.41	0	23.07	73.96
Learn from Scratch	42.41	0	23.07	68.85
Head-Tuning	0	0	23.07	62.45
Ours	0	2.22	23.07	72.17

the backbone of other methods are initialized with the model weights pre-trained on the large-scale ImageNet dataset (Deng et al. 2009). More backbone networks are explored in the ablation studies.

- **Head Segmenter.** For ADE20K and Vaihingen, we use Pyramid Pooling Module (PPM (Zhao et al. 2017)) as the head segmenter, since it has a great capacity to capture the scale variations of objects. For the three medical datasets, we use the Progressive UPsampling (PUP (Zheng et al. 2021)) head due to the fact that retinal vessels are very thin and we require high-resolution segmentation results for medical diagnosis. The parameters of all heads are randomly initialized.
- **Semantic-aware Prompt Matcher.** Based on its architecture, the ImageNet-pretrained ResNet-101 is divided into four stages. In our model, the proposed SPM is inserted before each stage and head segmenter to learn visual prompts. The feature channel  $\hat{c}$  in SPM is set to 256.
- **Implementation Details.** We apply MMSegmentation (Contributors 2020) to implement our experiments on 4 Nvidia GeForce 3090 GPUs. We train the models for 80k iterations with a batch size of 16 for the ADE20K and Vaihingen datasets. For the three medical datasets, we train the models for 40k iterations with a batch size of 4, due to the small amount of training data.

**Large-scale natural image segmentation** Table 2 shows the performance of different methods on the ADE20K dataset. We can observe that *full-tuning* obtains the best mIoU of 43.96%, much outperforming *learn-from-scratch* with the same number of trainable parameters, since the pre-trained backbone contains rich prior knowledge. When the backbone is frozen, *head-tuning* gets an mIoU of 34.08%. In contrast, our method can achieve a promising mIoU of 40.01%, by using a small amount of 3.11M parameters to learn visual prompts between frozen stages. This result is

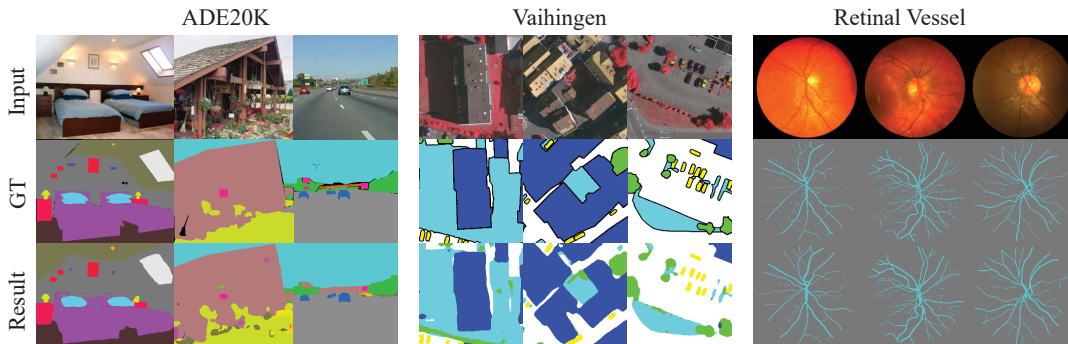


Figure 4: Visualization of the results of the proposed method. Using the same frozen backbone network, our method can generate high-quality semantic maps for natural, satellite, and medical image segmentation.

Table 4: The foreground Dice Similarity Coefficient (Dice) of different methods on three medical image semantic segmentation datasets. Except *Learn-from-Scratch*, the backbone of all methods is the ResNet-101 model pre-trained on ImageNet.

Method	Trainable Parameters (M)			Dice $\uparrow$		
	Backbone	Prompt	Head	Chase-dbl	Stare	HRF
Full-Tuning	42.41	0	5.90	79.94	80.74	80.75
Learn from Scratch	42.41	0	5.90	79.80	80.89	80.73
Head-Tuning	0	0	5.90	68.24	63.94	77.12
Ours	0	2.54	5.90	79.57	80.49	80.40

significantly better than that of *head-tuning* and also comparable with that of *full-tuning*. Figure 4 also shows that our method can generate high-quality semantic maps for unconstrained natural scenes.

**Medium-scale satellite image segmentation** Table 3 summarizes the results of all methods on the Vaihingen dataset. We see that the compared results on this dataset are very consistent with that on the ADE20K dataset. More specifically, *full-tuning* still obtains the best performance with a mIoU of 73.96%. When freezing the backbone and using 2.22M trainable parameters for prompt learning, our method achieves a competitive mIoU of 72.17%, significantly outperforming *learn-from-scratch* and *head-tuning*. This shows the great potential of our method for medium-scale image segmentation.

**Few-shot medical image segmentation** Table 4 shows the segmentation results on three retinal segmentation datasets. Compared with *head-tuning*, our method achieves significant improvements on all datasets via a small number of prompt learning parameters. On these few-shot datasets, we notice that *full-tuning*, *learn-from-scratch* and our method can obtain the best performance, but the first two approaches rely on a large number of trainable parameters to fit the data distribution. In this situation, one of the major advantages of our method is that the frozen backbone can be shared for semantic segmentation in various scenarios.

## Ablation Studies

**Effects of different pre-trained datasets** In this subsection, we explore the effect of pre-training data from the

Table 5: Performance of different methods on the ADE20K dataset when the backbone network was pre-trained on the COCO-Stuff-164k dataset.

Method	Trainable Parameters (M)			mIoU $\uparrow$
	Backbone	Prompt	Head	
Full-Tuning	42.41	0	23.15	43.47
Learn from Scratch	42.41	0	23.15	34.84
Head-Tuning	0	0	23.15	40.21
Ours	0	1.78	23.15	42.11

source domain. Specifically, we reimplement the experiments for the ADE20K dataset using a ResNet-101 model pre-trained on the COCO-Stuff-164K dataset (Caesar, Uijlings, and Ferrari 2018), which is another large-scale semantic segmentation benchmark. As shown in Table 5, using massive task-related data for pre-training can effectively contribute the performance of downstream tasks. Comparing the results of using ImageNet pre-trained backbone in Table 2, we observe that our method can achieve a better mIoU of 42.11% by using fewer prompt learning parameters (1.78M). This indicates that choosing models pre-trained on a proper source domain can be important. However, in practice many downstream tasks do not have large-scale datasets, so it makes sense to adopt the foundation models pre-trained on the ImageNet dataset.

**Effects of different prompted stages** We further explore the effects of inserting the proposed SPM into varied stages of the backbone model. As mentioned above, ResNet-101 consists of 4 stages and the head segmenter is treated as the 5th stage. As shown in Table 6, our performance grad-



Table 6: Performance of different prompted stages on the ADE20K dataset. +1 and +2 denote adding extra SPM to the interior of the 3rd stage of ResNet-101.

Prompted Stages	Prompted Parameters (M)	Pre-trained Dataset	
		ImageNet	COCO
1	0.48	34.43	40.89
1-2	1.07	35.11	41.74
1-3	1.78	36.39	<b>42.11</b>
1-4	2.36	38.54	41.74
1-5	3.11	40.01	42.10
1-5 (+1)	3.69	41.23	-
1-5 (+2)	4.27	<b>41.32</b>	-

Table 7: Performance of our method with/without semantic-aware prompt learning and long-range spatial context modeling on the ADE20K dataset.

Method	Pre-trained Dataset	
	ImageNet	COCO
w/o semantic-aware	38.08	41.10
w/o long-range context	39.25	41.66
Ours	40.01	42.11

ually increases as the number of prompted stages increases. Specifically, our method can achieve competitive results by using five SPM on the ImageNet pre-trained model and three SPM on the model pre-trained with COCO-Stuff-164K. In particular, we can further improve the performance of the ImageNet pre-trained model using more SPM. Notice that the 3rd stage of ResNet-101 has 23 residual units and we evenly split this stage into extra sub-stages for prompt learning, where +1 means inserting an SPM at the 12th units while +2 denotes inserting two SPM at 7th and 14th units, as shown in Table 6. The ImageNet pre-trained model reaches an optimal mIoU 41.32% with seven SPM. In general, more prompted stages lead to better results to a certain extent and the good pre-trained models need fewer prompt learning modules.

**Effects of semantic-aware prompt learning** In our SPM, interim semantic maps are incorporated to learn visual prompts at different stages. We ablate this model design by removing the semantic-aware module, i.e., all loss weights  $a_i$  in Eq. 5 are set to 0 during training. Table 7(Row 1) shows that without the semantic-aware will lead to inferior performance than using the semantic-aware. This experiment illustrates that the prior information of interim semantic maps is beneficial for effective prompt learning.

**Effects of long-range spatial context** We further explore the effectiveness of long-range spatial context modeling. To this end, we implement a variant of SPM that does not explicitly capture long-range context by replacing the Pyramid Dilation Convolution to a common convolutional layer with a kernel size of  $3 \times 3$ . As shown in Table 7(Row 2), there is a performance drop when PDC is replaced. This indicates that the long-range context is meaningful for semantic segmentation prompt learning.

Table 8: Performance of different methods on the ADE20K dataset, when the backbone network is ResNet50 pre-trained on ImageNet.

Method	Trainable Parameters (M)			mIoU $\uparrow$
	Backbone	Prompt	Head	
Full-Tuning	23.47	0	23.15	41.19
Learn from Scratch	23.47	0	23.15	32.83
Head-Tuning	0	0	23.15	33.26
Ours	0	3.11	23.15	37.64

Table 9: Performance of different methods on the ADE20K dataset when the backbone network is Vision-Transformer (ViT-L) pre-trained on ImageNet.

Method	Trainable Parameters (M)			mIoU $\uparrow$
	Backbone	Prompt	Head	
Full-Tuning	304.15	0	13.14	47.53
Head-Tuning	0	0	13.14	37.77
Ours (1 stage)	0	0.59	13.14	42.23
Ours (2 stages)	0	1.17	13.14	42.71
Ours (3 stages)	0	1.76	13.14	43.03

**Effects of different backbones** Finally, we investigate the effects of different backbone model sizes. Table summarizes the performance of different methods when using the smaller backbone model ResNet-50. We can observe that their results on ResNet-50 are consistent with those on ResNet-101. With fewer learned parameters of five SPM, our method obtains a mIoU of 37.64 on the ADE20K dataset, much outperforming *learn-from-scratch* and comparable to *full-tuning*.

We also apply the proposed method to fine-tune the large-scale backbone Vision-Transformer (ViT-L) (Zheng et al. 2021) with a batch size of 8. Notice that ViT-L consists of 24 transformer units and we evenly split these units into  $N$  stages, where  $N$  is set to 1, 2, and 3 in Table 9. We can see that our method achieves a very competitive mIoU 42.11% when using three SPM with 1.78M parameters to learn visual prompts. This experiment shows that the proposed method is also effective and efficient for transformer architecture.

## Conclusion

In this paper, we propose an Inter-Stage Prompt-Matched Framework for effective and parameter efficient fine-tuning large models to various semantic segmentation tasks. We conduct extensive experiments on five benchmark datasets to validate the tailor-designed Semantic-aware Prompt Matcher (SPM) regarding effectiveness and parameter efficiency of our proposed method. Results indicate that our method tend to benefit more from larger pre-trained backbone model. While the performance is also affected by other factors such as the pre-training datasets, the number of stages inserting our SPM, and the downstream task segmenter, etc. In the future, we will consider other pre-training strategies (Radford et al. 2021) and parameter efficient transfer learning techniques (He et al. 2021) to advance our proposed model.

## References

- Brown, T.; Mann, B.; Ryder, N.; Subbiah, M.; Kaplan, J. D.; Dhariwal, P.; Neelakantan, A.; Shyam, P.; Sastry, G.; Askell, A.; et al. 2020. Language models are few-shot learners. *Advances in neural information processing systems*, 33: 1877–1901.
- Budai, A.; Bock, R.; Maier, A.; Hornegger, J.; and Michelson, G. 2013. Robust vessel segmentation in fundus images. *International journal of biomedical imaging*, 2013.
- Caesar, H.; Uijlings, J.; and Ferrari, V. 2018. Coco-stuff: Thing and stuff classes in context. In *Proceedings of the IEEE conference on computer vision and pattern recognition*, 1209–1218.
- Chen, L.-C.; Papandreou, G.; Kokkinos, I.; Murphy, K.; and Yuille, A. L. 2015. Semantic Image Segmentation with Deep Convolutional Nets and Fully Connected CRFs. In *ICLR*.
- Chen, L.-C.; Papandreou, G.; Kokkinos, I.; Murphy, K.; and Yuille, A. L. 2017. Deeplab: Semantic image segmentation with deep convolutional nets, atrous convolution, and fully connected crfs. *IEEE transactions on pattern analysis and machine intelligence*, 40(4): 834–848.
- Chen, S.; Ge, C.; Tong, Z.; Wang, J.; Song, Y.; Wang, J.; and Luo, P. 2022. AdaptFormer: Adapting Vision Transformers for Scalable Visual Recognition. *arXiv preprint arXiv:2205.13535*.
- Contributors, M. 2020. MMSegmentation: OpenMMLab Semantic Segmentation Toolbox and Benchmark. <https://github.com/open-mmlab/mms Segmentation>.
- Deng, J.; Dong, W.; Socher, R.; Li, L.-J.; Li, K.; and Fei-Fei, L. 2009. Imagenet: A large-scale hierarchical image database. In *IEEE conference on computer vision and pattern recognition*, 248–255. IEEE.
- Devlin, J.; Chang, M.-W.; Lee, K.; and Toutanova, K. 2018. Bert: Pre-training of deep bidirectional transformers for language understanding. *arXiv preprint arXiv:1810.04805*.
- Dosovitskiy, A.; Beyer, L.; Kolesnikov, A.; Weissenborn, D.; Zhai, X.; Unterthiner, T.; Dehghani, M.; Minderer, M.; Heigold, G.; Gelly, S.; et al. 2020. An image is worth 16x16 words: Transformers for image recognition at scale. *arXiv preprint arXiv:2010.11929*.
- Fraz, M. M.; Remagnino, P.; Hoppe, A.; Uyyanonvara, B.; Rudnicka, A. R.; Owen, C. G.; and Barman, S. A. 2012. An ensemble classification-based approach applied to retinal blood vessel segmentation. *IEEE Transactions on Biomedical Engineering*, 59(9): 2538–2548.
- Fu, J.; Liu, J.; Tian, H.; Li, Y.; Bao, Y.; Fang, Z.; and Lu, H. 2019. Dual attention network for scene segmentation. In *Proceedings of the IEEE/CVF conference on computer vision and pattern recognition*, 3146–3154.
- He, J.; Deng, Z.; Zhou, L.; Wang, Y.; and Qiao, Y. 2019a. Adaptive pyramid context network for semantic segmentation. In *IEEE Conference on Computer Vision and Pattern Recognition*, 7519–7528.
- He, J.; Zhou, C.; Ma, X.; Berg-Kirkpatrick, T.; and Neubig, G. 2021. Towards a Unified View of Parameter-Efficient Transfer Learning. In *International Conference on Learning Representations*.
- He, K.; Zhang, X.; Ren, S.; and Sun, J. 2016. Deep residual learning for image recognition. In *Proceedings of the IEEE conference on computer vision and pattern recognition*, 770–778.
- He, X.; Yang, S.; Li, G.; Li, H.; Chang, H.; and Yu, Y. 2019b. Non-local context encoder: Robust biomedical image segmentation against adversarial attacks. In *Proceedings of the AAAI Conference on Artificial Intelligence*, volume 33, 8417–8424.
- He, Z.; Rakin, A. S.; and Fan, D. 2019. Parametric noise injection: Trainable randomness to improve deep neural network robustness against adversarial attack. In *Proceedings of the IEEE/CVF Conference on Computer Vision and Pattern Recognition*, 588–597.
- Hoover, A.; Kouznetsova, V.; and Goldbaum, M. 2000. Locating blood vessels in retinal images by piecewise threshold probing of a matched filter response. *IEEE Transactions on Medical imaging*, 19(3): 203–210.
- Hu, S.; Ding, N.; Wang, H.; Liu, Z.; Wang, J.; Li, J.; Wu, W.; and Sun, M. 2022. Knowledgeable Prompt-tuning: Incorporating Knowledge into Prompt Verbalizer for Text Classification. In *Proceedings of the Annual Meeting of the Association for Computational Linguistics*, 2225–2240.
- Jia, C.; Yang, Y.; Xia, Y.; Chen, Y.-T.; Parekh, Z.; Pham, H.; Le, Q.; Sung, Y.-H.; Li, Z.; and Duerig, T. 2021. Scaling up visual and vision-language representation learning with noisy text supervision. In *International Conference on Machine Learning*, 4904–4916. PMLR.
- Jia, M.; Tang, L.; Chen, B.-C.; Cardie, C.; Belongie, S.; Hariharan, B.; and Lim, S.-N. 2022. Visual prompt tuning. *arXiv preprint arXiv:2203.12119*.
- Liao, F.; Liang, M.; Dong, Y.; Pang, T.; Hu, X.; and Zhu, J. 2018. Defense against adversarial attacks using high-level representation guided denoiser. In *Proceedings of the IEEE conference on computer vision and pattern recognition*, 1778–1787.
- Liu, L.; Yang, Z.; Li, G.; Wang, K.; Chen, T.; and Lin, L. 2022. Aerial images meet crowdsourced trajectories: a new approach to robust road extraction. *IEEE transactions on neural networks and learning systems*.
- Liu, P.; Yuan, W.; Fu, J.; Jiang, Z.; Hayashi, H.; and Neubig, G. 2021. Pre-train, prompt, and predict: A systematic survey of prompting methods in natural language processing. *arXiv preprint arXiv:2107.13586*.
- Long, J.; Shelhamer, E.; and Darrell, T. 2015. Fully convolutional networks for semantic segmentation. In *Proceedings of the IEEE conference on computer vision and pattern recognition*, 3431–3440.
- Ma, Y.; Kim, M.; Cao, Y.; Vrudhula, S.; and Seo, J.-s. 2017. End-to-end scalable FPGA accelerator for deep residual networks. In *IEEE International Symposium on Circuits and Systems*, 1–4. IEEE.
- Madry, A.; Makelov, A.; Schmidt, L.; Tsipras, D.; and Vladu, A. 2018. Towards Deep Learning Models Resistant to Adversarial Attacks. In *International Conference on Learning Representations*.



- Minaee, S.; Boykov, Y. Y.; Porikli, F.; Plaza, A. J.; Kehtarnavaz, N.; and Terzopoulos, D. 2021. Image segmentation using deep learning: A survey. *IEEE transactions on pattern analysis and machine intelligence*.
- Nurvitadhi, E.; Sim, J.; Sheffield, D.; Mishra, A.; Krishnan, S.; and Marr, D. 2016. Accelerating recurrent neural networks in analytics servers: Comparison of FPGA, CPU, GPU, and ASIC. In *International Conference on Field Programmable Logic and Applications*, 1–4. IEEE.
- Radford, A.; Kim, J. W.; Hallacy, C.; Ramesh, A.; Goh, G.; Agarwal, S.; Sastry, G.; Askell, A.; Mishkin, P.; Clark, J.; et al. 2021. Learning transferable visual models from natural language supervision. In *International Conference on Machine Learning*, 8748–8763. PMLR.
- Ronneberger, O.; Fischer, P.; and Brox, T. 2015. U-net: Convolutional networks for biomedical image segmentation. In *International Conference on Medical image computing and computer-assisted intervention*, 234–241. Springer.
- Strudel, R.; Garcia, R.; Laptev, I.; and Schmid, C. 2021. Segmenter: Transformer for semantic segmentation. In *Proceedings of the IEEE/CVF International Conference on Computer Vision*, 7262–7272.
- Tan, Z.; Zhang, X.; Wang, S.; and Liu, Y. 2022. MSP: Multi-Stage Prompting for Making Pre-trained Language Models Better Translators. In *Proceedings of the 60th Annual Meeting of the Association for Computational Linguistics (Volume 1: Long Papers)*, 6131–6142.
- Vaswani, A.; Shazeer, N.; Parmar, N.; Uszkoreit, J.; Jones, L.; Gomez, A. N.; Kaiser, Ł.; and Polosukhin, I. 2017. Attention is all you need. *Advances in neural information processing systems*, 30.
- Wang, Y.; Qin, Y.; Deng, D.; Wei, J.; Zhou, Y.; Fan, Y.; Chen, T.; Sun, H.; Liu, L.; Wei, S.; et al. 2022. A 28nm 27.5 TOPS/W Approximate-Computing-Based Transformer Processor with Asymptotic Sparsity Speculating and Out-of-Order Computing. In *IEEE International Solid-State Circuits Conference*, volume 65, 1–3. IEEE.
- Yang, Z.; Gan, Z.; Wang, J.; Hu, X.; Lu, Y.; Liu, Z.; and Wang, L. 2022. An empirical study of gpt-3 for few-shot knowledge-based vqa. In *Proceedings of the AAAI Conference on Artificial Intelligence*, volume 36, 3081–3089.
- Zeng, W.; Ren, X.; Su, T.; Wang, H.; Liao, Y.; Wang, Z.; Jiang, X.; Yang, Z.; Wang, K.; Zhang, X.; et al. 2021. PanGu- $\alpha$ : Large-scale Autoregressive Pretrained Chinese Language Models with Auto-parallel Computation. *arXiv preprint arXiv:2104.12369*.
- Zhao, H.; Shi, J.; Qi, X.; Wang, X.; and Jia, J. 2017. Pyramid scene parsing network. In *IEEE conference on computer vision and pattern recognition*, 2881–2890.
- Zheng, S.; Lu, J.; Zhao, H.; Zhu, X.; Luo, Z.; Wang, Y.; Fu, Y.; Feng, J.; Xiang, T.; Torr, P. H.; et al. 2021. Rethinking semantic segmentation from a sequence-to-sequence perspective with transformers. In *Proceedings of the IEEE/CVF conference on computer vision and pattern recognition*, 6881–6890.
- Zhou, B.; Zhao, H.; Puig, X.; Fidler, S.; Barriuso, A.; and Torralba, A. 2017. Scene parsing through ade20k dataset. In *Proceedings of the IEEE conference on computer vision and pattern recognition*, 633–641.
- Zhu, Z.; Xu, M.; Bai, S.; Huang, T.; and Bai, X. 2019. Asymmetric non-local neural networks for semantic segmentation. In *IEEE International Conference on Computer Vision*, 593–602.